

COHmax: An algorithm to maximise coherence in estimates of dynamic cerebral autoregulation

Ronney B Panerai^{1,2}, Kannakorn Intharakham¹, Jatinder S Minhas^{1,2}, Osian Llwyd¹, Angela S M Salinet³, Emmanuel Katsogridakis⁴, Paola Maggio⁵, and Thompson G Robinson^{1,2}

¹ Cerebral Haemodynamics in Ageing and Stroke Medicine (CHiASM) Research Group, Department of Cardiovascular Sciences, University of Leicester, Leicester, United Kingdom

² NIHR Leicester Biomedical Research Centre, British Heart Foundation Cardiovascular Research Centre, Glenfield Hospital, Leicester, UK

³ Neurology Department, Hospital das Clinicas, School of Medicine, University of Sao Paulo, Sao Paulo, Brazil

⁴ Department of Vascular Surgery, Wythenshawe Hospital, Manchester Foundation Trust, Manchester, UK

⁵ Neurology Department, ASST Bergamo EST(BG), Italy

Corresponding author

RB Panerai
Department of Cardiovascular Sciences, University of Leicester
Sir Robert Kilpatrick Clinical Sciences Building, Leicester Royal Infirmary
Leicester LE2 7LX, UK
E-mail: rp9@le.ac.uk
Tel. +44(0)1162523130

Abstract

Objective. The reliability of dynamic cerebral autoregulation (dCA) parameters, obtained with transfer function analysis (TFA) of spontaneous fluctuations in arterial blood pressure (BP), require statistically significant values of the coherence function. A new algorithm (COH_{max}) is proposed to increase values of coherence by means of the automated, selective removal of sub-segments of data.

Approach. Healthy subjects were studied at baseline (normocapnia) and during 5% breathing of CO_2 (hypercapnia). BP (Finapres), cerebral blood flow velocity (CBFV, transcranial Doppler), end-tidal CO_2 (EtCO_2 , capnography) and heart rate (ECG) were recorded continuously during 5 min in each condition. TFA was performed with sub-segments of data of duration (SEG_D) 100, 50 or 25 s and the autoregulation index (ARI) was obtained from the CBFV response to a step change in BP. The area-under-the curve (AUC) was obtained from the receiver-operating characteristic (ROC) curve for the detection of changes in dCA resulting from hypercapnia.

Main results. In 120 healthy subjects (69 male, age range 20-77 years), CO_2 breathing was effective in changing mean EtCO_2 and CBFV ($p < 0.001$). For $\text{SEG}_D = 100$ s, ARI changed from 5.8 ± 1.4 (normocapnia) to 4.0 ± 1.7 (hypercapnia, $p < 0.0001$), with similar differences for $\text{SEG}_D = 50$ or 25 s. Depending on the value of SEG_D , in normocapnia, 15.8% to 18.3% of ARI estimates were rejected due to poor coherence, with corresponding rates of 8.3% to 13.3% in hypercapnia. With increasing coherence, 36.4% to 63.2% of these could be recovered in normocapnia ($p < 0.001$) and 50.0% to 83.0% in hypercapnia ($p < 0.005$). For $\text{SEG}_D = 100$ s, ROC AUC was not influenced by the algorithm, but it was superior to corresponding values for $\text{SEG}_D = 50$ or 25 s.

Significance. COH_{max} has the potential to improve the yield of TFA estimates of dCA parameters, without introducing a bias or deterioration of their ability to detect impairment of autoregulation. Further studies are needed to assess the behaviour of the algorithm in patients with different cerebrovascular conditions.

Keywords: cerebral blood flow, transfer function analysis, autoregulation index, receiver operator characteristic curve

1. Introduction

The concept of dynamic cerebral autoregulation (dCA) is based on the tendency of cerebral blood flow (CBF) to return to its original value following a transient disturbance, provoked by a sudden change in arterial blood pressure (BP). Although dCA was initially assessed in studies where a rapid drop in BP was induced by the sudden deflation of pressurised thigh cuffs (Aaslid et al. 1989), subsequently, a number of alternative approaches have been proposed, whose merits and limitations are still being debated (Simpson and Claassen 2018; Tzeng and Panerai 2018). Chiefly amongst these different possibilities, is the use of spontaneous fluctuations in BP as the stimulus to induce corresponding changes in CBF (Tzeng and Panerai 2018). Spontaneous changes in BP can be treated as isolated transients (Panerai et al. 2003; Panerai et al. 1995), or, more commonly, as the input function in transfer function analysis (TFA), where corresponding changes in CBF, or CBF velocity (CBFV) are regarded as the output function (Claassen et al. 2016; Giller 1990; Panerai et al. 1996; Zhang et al. 1998). On one hand, the use of TFA in combination with spontaneous fluctuations in BP is the ideal approach in clinical studies, since the necessary noninvasive physiological measurements can be performed in critically ill patients, something that is not feasible with other methods (e.g. changes in posture), and it also minimises disturbances to ongoing physiological processes. On the other hand though, its reliability has been questioned, mainly due to its poor reproducibility and susceptibility to nonstationarity (Panerai 2013; Sanders et al. 2018; Sanders et al. 2019; Simpson and Claassen 2018).

Given its widespread utilization as a tool for clinical assessment of dCA, TFA of spontaneous fluctuations in BP deserves further attention to overcome its limitations. A recent White Paper from the International Cerebral Autoregulation Research Network (CARNet) is likely to lead to improvements resulting from greater standardisation (Claassen et al. 2016). Limited BP variability has also been suggested as the cause of poor reproducibility observed with the classical parameters extracted by TFA to characterise dCA, such as the gain, phase and the autoregulation index (ARI) (Liu et al. 2005; Panerai et al. 1998b; Simpson and Claassen 2018; Tiecks et al.

1995; Zhang et al. 1998). Recent work has demonstrated removal of recordings with low BP variability can lead to improvements in reproducibility (Elting et al. 2020).

A further possibility for improving the reliability of TFA estimates of dCA, is by boosting the coherence of the BP-CBF transfer function. At each frequency, coherence represents the fraction of output power (i.e. CBF/CBFV) that is linearly explained by the input power (i.e. BP). Therefore, similar to a correlation coefficient, coherence ranges between zero and one, with values approaching one in the case of a linear, univariate relationship between BP and CBF, and measurements devoid of noise. Coherence will tend towards zero when the signal-to-noise ratio (SNR) is poor, there are multiple determinants of CBF, or if the relationship with BP is highly nonlinear (Bendat and Piersol 1986). Although initially proposed as a metric of dCA efficiency (Giller 1990), the main use of coherence in TFA studies of dCA has been as an indicator of the reliability of gain and phase estimates. At each frequency, estimates of gain and phase should only be accepted if the corresponding values of coherence are statistically significant; this criterion being usually based on the 95% confidence limit of coherence for the null hypothesis (Benignus 1969; Claassen et al. 2016; Panerai et al. 2018). In clinical studies, rejecting estimates of gain and phase at different frequencies, where coherence is below the 95% confidence limit threshold, is problematic as it would lead to incomplete sets of data with different subsets of harmonics represented in different patients. An important alternative to this approach is to use all the information contained in the gain and phase frequency responses, as reflected by the ARI (Tiecks et al. 1995). The ARI ranges from 0 (absence of autoregulation) to 9 (best dCA that can be observed) and can be derived from the CBF/CBFV step response to the BP input, calculated from the inverse fast Fourier response of the gain and phase (Panerai et al. 1998b). With this approach, coherence can still be used as a marker of reliability, with values below the 95% confidence limit leading to the rejection of estimates of ARI (Panerai et al. 2018; Panerai et al. 2016). The challenges of performing measurements in a clinical environment usually lead to worse SNR and poorer values of coherence in patients when compared to healthy controls. To address this problem, we present a new algorithm for estimation of ARI, aimed at maximising values of coherence by automated, selective removal of sub-segments of data. In other words, we

tested the hypothesis that improvements in TFA coherence will lead to greater sensitivity and specificity for detection of dCA deterioration, as assessed with ARI. Although motivated by the need to improve the reliability of dCA metrics, this new algorithm would also be applicable to other areas of physiological measurement using TFA, such as estimates of baroreceptor sensitivity (Robbe et al. 1987) or heart rate variability (Saul et al. 1991).

2. Methods

2.1 Subjects and measurements

Participants were healthy subjects, recruited in four previous studies where hypercapnia was induced by 5% CO₂ breathing in air. All studies had local Ethical Committee approval and all participants provided written informed consent (Katsogridakis et al. 2013; Llwyd et al. 2017; Maggio et al. 2013; Minhas et al. 2018). Subjects were 18 years of age or older without any history or symptoms of cardiovascular, neurological or respiratory disease.

Volunteers avoided caffeine, alcohol, and nicotine for ≥ 4 h before attending a research laboratory with controlled temperature (20-23°C) and free from visual or auditory stimulation. All recordings were performed with subjects in the supine position with the head elevated at 30°. Following instrumentation and a 20 min rest, two 5 min recordings were performed in each subject. The first recording corresponded to baseline resting conditions with subjects breathing ambient air. In the second recording, after a 60 s period of breathing air, subjects were switched to breathing 5% CO₂ in air, through a face mask that was tightly fitted to avoid leakage, as confirmed by visual inspection of the end-tidal CO₂ waveform. After three min of CO₂ breathing, subjects were returned to ambient air and a further 60 s was recorded during return to normocapnia.

BP was recorded continuously using a Finapres/Finometer device (FMS, Finapres Measurement Systems, Arnhem, Netherlands), attached to the middle finger of the left hand. Systolic and diastolic BP were measured by classical brachial sphygmomanometry before each 5 min recording. Heart rate was derived from a 3-lead electrocardiogram (ECG). End-tidal CO₂ (EtCO₂)

was recorded continuously via nasal prongs (Salter Labs) by a capnograph (Capnocheck Plus). CBFV was measured in both middle cerebral arteries (MCAs) using transcranial Doppler ultrasound (TCD, Viasys Companion III; Viasys Healthcare) with 2 MHz probes secured in place using a head-frame. The servo-correcting mechanism of the Finapres/Finometer was switched on and then off prior to measurements.

Data were simultaneously recorded onto a data acquisition system (PHYSIDAS, Department of Medical Physics, University Hospitals of Leicester) for subsequent off-line analysis using a sampling rate of 500 samples/s.

2.3 Data analysis

All signals were visually inspected to identify artefacts; noise and narrow spikes (<100 ms) were removed by linear interpolation. CBFV channels were subjected to a median filter and all signals were low-pass filtered with a 8th order Butterworth filter with cut-off frequency of 20 Hz. BP was calibrated at the start of each recording using systolic and diastolic values obtained with sphygmomanometry. The R–R interval was then automatically marked from the ECG and beat-to-beat heart rate (HR) was plotted against time. Occasional missed marks caused spikes in the HR signal; these were manually removed by remarking the R–R intervals for the time points at which they occurred. Mean, systolic and diastolic BP and CBFV values were calculated for each cardiac cycle. The end of each expiratory phase was detected in the EtCO₂ signal, linearly interpolated, and resampled with each cardiac cycle. Beat-to-beat data were spline interpolated and resampled at 5 samples/s to produce signals with a uniform time-base.

In-house software, implemented in Fortran, was used to perform TFA of the BP-CBFV relationship using Welch's method (Welch 1967) with different combinations of segment durations (SEG_D) as described below. The mean values of BP and CBFV were removed from each segment and a cosine window was applied to minimise spectral leakage. The squared coherence function, amplitude (gain) and phase frequency responses were calculated from the smoothed auto- and cross-spectra using standard procedures (Claassen et al. 2016; Panerai et al. 1998a). The CBFV impulse response to the BP input was estimated using the inverse fast Fourier transform of gain and phase (Bendat and Piersol 1986) and the corresponding step response was

obtained by numerical integration for positive values of time. Tiecks et al (Tiecks et al. 1995) proposed 10 template curves for the CBFV response to a step change in BP, each of these curves corresponding to a value of ARI, ranging from 0 to 9. For each recording, the corresponding value of ARI was estimated by comparing the CBFV step response with each of the template curves and choosing the best fit using the normalised minimum square error (NMSE). ARI values were only accepted if the mean squared coherence function for the 0.15-0.25 Hz frequency interval (see Discussion) was above its 95% confidence limit, adjusted for the corresponding degrees of freedom (Panerai et al. 2020), and the NMSE was ≤ 0.30 (Panerai et al. 2016).

COH_{max} algorithm

For each 5 min recording, increasing values of coherence were obtained according to the following procedure:

- i) A *Reference Setting* condition was initially adopted to estimate coherence using all segments available in the 5 min recording with SEG_D settings of 102.4, 51.2 or 25.6 s (Claassen et al. 2016; Panerai et al. 2020). With a sampling rate of 5 samples/s, these durations corresponded to N_w = 512, 256 or 128 samples, respectively. In what follows, values of SEG_D will be referred to as 100, 50 and 25 s, respectively, for simplicity. With 50% superposition of segments, the number of segments (N_{SEG}) used to obtain estimates of the BP and CBFV auto- and cross-spectra were 5, 11 and 23, for SEG_D values of 100, 50 and 25 s, respectively. For each value of SEG_D, a receiver-operating characteristic (ROC) curve analysis was performed for the detection of changes in ARI due to hypercapnia, in comparison with corresponding values of normocapnia. The area-under-the-curve (AUC) was calculated for statistical testing of differences between ROC curves resulting from increases in coherence.
- ii) For each setting of SEG_D, the corresponding N_{SEG} segments were assigned at fixed positions along the 5 min recording, that is, in sequential fashion, also taking into consideration the 50% superposition of segments.

- iii*) At each step $j=1, 2, \dots, N_{\text{SEG}}-2$ data segments were removed one at a time and the coherence was recalculated for all combinations of the remaining $N_{\text{SEG}}-j$ segments. The segment corresponding to the combination with the lowest coherence was removed from the ensemble and the number of segments was reset to $N_{\text{SEG}}-j$. The coherence, ARI index and AUC were re-calculated and their dependence on the number of segments was expressed as $COH(N_{\text{SEG}})$ and $ARI(N_{\text{SEG}})$, and $AUC(N_{\text{SEG}})$, respectively.
- iv*) Stage (*iii*) above was repeated until only two segments remained.

In summary, for each setting of SEG_D (100s, 50s, or 25s), a total of $N_{\text{SEG}}-1$ estimates of coherence, ARI and AUC were obtained, corresponding to 4, 10 and 22 values in each setting, respectively, including the *Reference Setting* values obtained from (*i*) above.

2.4 Statistical analysis

Data were treated as normally distributed after visual inspection of histograms and probability plots, taking into consideration the large size of the sample ($n>100$) studied. Differences between parameters were assessed using the Student's t -test. Multiple parameter comparisons were performed with parametric repeated-measures ANOVA. Differences between values derived for the right and left hemispheres were averaged when no significant differences were found. Association between variables was tested with linear regression. For each value of N_{SEG} , the 95% confidence limits for coherence were obtained as reported previously (Claassen et al. 2016; Panerai et al. 2020). The improvement in ROC detection, due to increased values of $COH(N_{\text{SEG}})$ was assessed by testing the $AUC(N_{\text{SEG}})$ with the method proposed by DeLong et al. (DeLong et al. 1988). A p -value of < 0.05 was assumed to indicate statistical significance.

3. Results

One hundred and twenty healthy subjects (66 male), aged 43.2 ± 15.1 years old (range 20-77 years) provided a complete set of measurements for both baseline and hypercapnia. As shown in Table 1, highly significant differences were observed for EtCO₂ and CBFV, as well as for BP and HR between normocapnia and hypercapnia. No inter-hemispherical differences were found for any of the parameters studied, which were then averaged for the right and left MCA.

According to its design, COH_{max} led to increases in coherence in all subjects, both during normocapnia and hypercapnia, but with different individual patterns, as illustrated in Fig. 1. For the population as a whole, increases in coherence were similar for normocapnia and hypercapnia (Figs. 2.A and B), with SEG_D = 25 s providing the highest mean values at N_{SEG} = 2, followed by SEG_D = 50 s and 100 s, respectively. In each case, the starting value of N_{SEG} was the *Reference Setting*, corresponding to 5, 11 and 23 segments, for SEG_D values of 100, 50 and 25 s, respectively. Noticeably, as the number of segments was reduced, so was the inter-subject variability as expressed by the standard errors in Fig. 2.

Despite marked increases in coherence resulting from COH_{max}, the mean ARI remained relatively stable (Figs 2.C and D), but showed highly significant differences due to hypercapnia and also due to SEG_D, but only for the case of SEG_D = 25 s (Table 2). The relative stability of ARI, as the number of segments was reduced with application of COH_{max}, can be expressed by the distributions of intra-subject standard deviations (SD_{ARI}^{intra} , Table 2) as depicted in Fig. 3, showing modes of ≤ 0.5 units in all cases. Correlation of SD_{ARI}^{intra} with the *Reference Setting* values of coherence were significant for SEG_D = 50 s ($p=0.0036$) and SEG_D = 25 s ($p=0.008$), but only for the hypercapnia condition. Assuming that coherence changed from 0.0 to 1.0, the corresponding expected improvement in SD_{ARI}^{intra} would be of approximately 50% in both cases. For SEG_D = 100 s, there was no significant association between coherence for the *Reference Setting* and SD_{ARI}^{intra} for either the normocapnic or hypercapnic conditions.

The number of values of ARI that were rejected due to the joint criteria, based on the 95% confidence limit for coherence and the NMSE, was relatively small (Table 3), but it still decreased

significantly with the use of COH_{max} . Both normocapnia ($p < 0.001$) and hypercapnia ($p < 0.005$) showed significant rates of improvement, but with a larger difference in hypercapnia as compared to normocapnia ($p = 0.03$).

ROC analysis led to relatively stable values of $AUC(N_{\text{SEG}})$ with gradual reductions in N_{SEG} along with increases in coherence resulting from COH_{max} (Fig. 4). In other words, for each value of SEG_D , coherence did not have an effect on $AUC(N_{\text{SEG}})$, but AUC values for $\text{SEG}_D = 100$ s were significantly higher than corresponding values for $\text{SEG}_D = 50$ s or 25 s (Fig. 4).

4. Discussion

4.1 Main findings

Despite the substantial increase in the computational effort required by the COH_{max} algorithm, there were no noticeable increases in execution time, in comparison with standard TFA analysis (Claassen et al. 2016), running on a 2.7 GHz personal computer in DOS mode. The feasibility of increasing coherence values, in the spectral region where a linear relationship between BP and CBFV would be expected (0.15-0.25 Hz), whilst still retaining enough BP and CBFV power to provide acceptable signal-to-noise ratio (Panerai et al. 2018), was well demonstrated by the steady increase in coherence shown in Fig. 2. Although the dataset analysed comprised high-quality recordings, with mean values of coherence well above its 95% confidence limit for the *Reference Setting* (Figs. 2A and B), a relatively small number of subjects showed coherence values below the 95% confidence limit (Fig. 1) that would lead to their rejection and impossibility of extracting corresponding values of ARI (Table 3). A significant number (15.8 % to 83.3%) of these recordings could be recovered with COH_{max} , showing its potential to contribute towards improving the use of dCA assessment in personalised patient care. Pertinent to the possibility of improving coherence by the selective, but automated removal of segments of data, the ARI index remained relatively stable (Figs 2A, 2B, 3) thus showing that the algorithm did not introduce any biases in its estimation, except at the lowest values of N_{SEG} for $\text{SEG}_D = 25$ s (Fig. 2C and D). On the other hand, our main hypothesis, that increases in coherence would lead to corresponding

improvements in the detection of worsening CA, as would be expected with hypercapnia (Aaslid et al. 1989; Minhas et al. 2018; Panerai et al. 1999), was rejected given that AUC remained relatively constant with increases in coherence (Fig. 4). Noteworthy, the AUC for $SEG_D = 100$ s was significantly higher than that observed for $SEG_D = 50$ s or 25 s (Fig. 4).

Taken together, our findings suggest that COH_{max} could be a useful tool to rescue recordings with unacceptable values of coherence in the *Reference Setting*, but without the expectation that it would necessarily lead to improvements in diagnostic discrimination, given that ARI values and corresponding ROC curves were broadly not affected by the algorithm.

4.2 Methodological considerations

TFA based on the Fourier transform, requires calculation of the auto- and cross-spectra (Bendat and Piersol 1986). With a single, long segment of data, e.g. 5 min duration, spectral estimates will show considerable variability, following a chi-square distribution with two degrees of freedom (DF), and a coefficient of variation of 1.0 (Bendat and Piersol 1986). To reduce the variance of spectral estimates and, consequently, the reliability of estimates of gain and phase, Welch proposed smoothing the auto- and cross-spectral estimates by averaging multiple segments of data from the original long recording, thus increasing the number of DF (Welch 1967). One additional benefit of this approach is the possibility of calculating the coherence function, something that is not possible with a single segment of data (Benignus 1969). One interesting feature of the Welch method is that the data segments used for smoothing the auto- and cross-spectra do not need to be contiguous. When breaking down a long recording into N_{SEG} segments with duration $[SEG_D, N_W]$, these are often shifted across and superimposed by a certain amount, typically 50% (Claassen et al. 2016), but in the final calculation of the smoothed spectra, it does not matter the order in which segments are selected. This property of the Welch method can be used to remove bad segments of data, or to focus on specific events in a longer recording (Panerai et al. 2005). In the present study, we benefitted from this property, to gradually remove automatically selected segments of data in order to increase the coherence of TFA for the dynamic BP-CBFV relationship. The vast majority of reports in the literature of dCA assessment by means of TFA include estimates of

coherence as a marker of the reliability of estimates of gain and phase, as well as the ARI index (Panerai et al. 2016). Although the threshold adopted for the minimum value of coherence that should be used for acceptance of TFA estimates has been fairly variable, ranging from 0.12 (for $N_{SEG}=15$) (Claassen et al. 2016) to 0.50 (for any N_{SEG}) (Zhang et al. 1998), the literature is unanimous that estimates of gain, phase and ARI (when obtained via TFA), should not be accepted below a pre-defined threshold of coherence. Ideally, this threshold should be based on the 95% confidence limit of the coherence distribution for the null hypothesis (or other value of $1-\alpha$) (Benignus 1969). For 5 min recordings, using $SEG_D = 100$ s and 50% superposition, the coherence threshold will be 0.34, for $\alpha = 0.05$ (Claassen et al. 2016). Complete curves of the 95% confidence limit as a function of N_{SEG} , have been reported for other values of SEG_D (Panerai et al. 2020).

Another common observation in the literature is the suggestion that the higher the coherence, the more reliable the estimates of gain and phase will be (Claassen et al. 2009; Smirl et al. 2015).

This assumption is understandable, given that poor coherence can be caused by low SNR, as well as by other factors, such as non-linearity and multiple influences on the output variable (i.e. CBFV). Accordingly, it should be expected that by increasing coherence, one would obtain improved estimates of gain and phase, and, by extension, of ARI calculated via TFA, leading to better diagnostic and/or prognostic accuracy. In this study, with values of coherence starting at ~ 0.65 (*Reference Setting*) and increasing to around 0.9 (Fig. 2), a substantial increase in coherence did not confirm those expectations, as reflected by the stable values of AUC shown in Fig. 4 and the lack of association between SD_{ARI}^{intra} and the coherence of the *Reference Setting* (with the exception of $SEG_D = 50$ s and 25 s in hypercapnia). This result can be explained on theoretical grounds. Both the relative error of gain, and the standard error of estimates of phase, are predicted to vary as $[(1-\gamma^2)/2\gamma^2N_{SEG}]^{1/2}$, where γ^2 is the squared coherence function as calculated in our study (Bendat and Piersol 1986). As coherence increases, the errors will tend to go down, but, in our case, this is achieved with a gradual reduction in N_{SEG} (Fig. 2) and, as a

result, the estimation errors for gain and phase tend to remain approximately constant, which would explain similar behaviour for ARI.

Further work is needed with other datasets to replicate our findings, ideally involving recordings where the mean coherence for the *Reference Setting* is much lower than what we obtained.

Another potential use of COH_{max} would be in studies of the nonstationarity of dCA (Panerai 2013). Recordings with high values of $\text{SD}_{\text{ARI}}^{\text{intra}}$ might reflect the presence of nonstationarity of dCA parameters, that could be caused by recording artefacts, variable levels of sensorimotor or cognitive stimulation, changes in breathing patterns, or unknown physiological processes (Panerai 2013). Nonstationarity of physiological origin is thought to be behind the poor reproducibility observed in most metrics of dCA (Elting et al. 2014; Sanders et al. 2019) and COH_{max} could be a useful tool to address this problem.

4.3 Clinical implications

The standard approach to assessment of the diagnostic or prognostic accuracy of a physiological measurement is the analysis of ROC curves as a global representation of its sensitivity and specificity for all possible thresholds to distinguish between two distinct groups of participants or different physiological conditions. ROC analysis has been applied in clinical studies of dCA, using several different metrics (Brady et al. 2008; Budohoski et al. 2012; Hu et al. 2008; Lam et al. 2019; Ono et al. 2012). For an index of dCA to discriminate between patient and control groups, there is an underlying assumption that all patients have impaired autoregulation, which is something that cannot be guaranteed, except in conditions where all patients are severely ill. To avoid the fallacies of this assumption, hypercapnia has been used as a surrogate for depressed dCA (Aaslid et al. 1989; Katsogridakis et al. 2013; Maggio et al. 2013; Minhas et al. 2018; Panerai et al. 1999), with the added benefit that each subject can act as their own control. In this study, hypercapnia led to significant depression of dCA (Figs 2C and D), as well as highly significant values of AUC, when compared to the null hypothesis of $\text{AUC}=0.5$ (Fig. 4). Nevertheless, the values of AUC we obtained were lower than corresponding values in the

literature, but those involved different physiological conditions (Katsogridakis et al. 2013), or more complex mathematical models (Chacon et al. 2018).

The finding that COH_{max} can rescue recordings that would be rejected with the *Reference Setting* (Table 3), without degrading of the ARI's ability to detect worsening of dCA, as reflected by the ROC AUC (Fig. 4), suggests it can be a useful tool to allow assessment of dCA in patients who otherwise would be denied this test. For patients who are sufficiently fit, improvements in coherence can be obtained with other protocols, such as the squat-stand manoeuvre (Claassen et al. 2009; Simpson and Claassen 2018; Smirl et al. 2014; Smirl et al. 2015), but for critically ill patients, or those who cannot tolerate changes in posture, or even mild exercise, assessment of dCA based on spontaneous fluctuations in BP is the main alternative (Tzeng and Panerai 2018), as demonstrated by the widespread use of this approach in stroke and severe head injury (Intharakham et al. 2019a; Rivera-Lara et al. 2017). In critically ill patients, or those with conditions such as Parkinson's disease, good quality recordings are much more challenging than those performed in healthy volunteers under ideal conditions. As a result, the likelihood of recordings with poor coherence in the *Reference Setting* condition is much greater than that found in our healthy group, leading to a much greater fraction of data rejection with the TFA approach. It is in this context that COH_{max} might prove of utility, but further work is needed with different populations to assess the extent of the benefit that can be derived.

The study also provided additional information that could benefit clinical applications of dCA assessment. The White Paper from CARNet (Claassen et al. 2016), has provided a number of recommendations for improving standardisation of TFA settings, aiming to improve comparability of studies and also as an essential requirement to expand multi-centre collaborations (Beishon et al. 2020). However, many of the recommendations of the White Paper were based more on preferences identified in the literature (Meel-van den Abeelen et al. 2014), than objective evidence (Claassen et al. 2016). This is the case with the recommendation to standardise the duration of recordings to 5 min, with the use of $\text{SEG}_D = 100$ s for TFA with Welch's method (Claassen et al. 2016). As mentioned above, in clinical applications of dCA assessment, good quality recordings lasting 5 min might not always be feasible. This concern led

to studies exploring alternative settings, such as shortening the duration of recordings (Intharakham et al. 2019b), or the use of different values of SEG_D (Panerai et al. 2020). As demonstrated in these studies, the possibility of using recordings with shorter durations, and also with different values of SEG_D , has endorsed the choice of considering values of SEG_D of 50 or 25 s in the present study. The new relevant finding though, is that the $SEG_D = 100$ s setting leads to significantly better values of AUC of ROC curves, in comparison with the other two alternatives (Fig. 4). Based on this result, it would be appropriate to strengthen the White Paper's recommendation for use of $SEG_D = 100$ s as a standard, and its use combined with COH_{max} in cases of poor coherence with the *Reference Setting*. Furthermore, in future clinical applications, it would also be relevant to assess the use of only a few segments of data, such as $N_{SEG}=2$ or 3, to confirm the feasibility of this option when no more segments of data are available with significant coherence (Fig. 2)

4.4 Limitations of the study

Hypercapnia has been shown to increase the diameter of the MCA, but at much higher levels of $PaCO_2$ than observed in this study (Coverdale et al. 2014; Verbree et al. 2014). One advantage of ARI, as compared to TFA gain, is that this index is not affected by amplitude changes in CBFV between recordings, but it would certainly result in distortions if CBFV were affected by intra-recording changes in MCA diameter.

Application of TFA to dynamic CA relies on the assumption that the BP-CBFV relationship is linear. As mentioned above, this assumption is not acceptable for frequencies below approximately 0.15 Hz because an active CA implies that cerebrovascular resistance is changing over time, thus representing a departure from the premise of linearity (Bendat and Piersol 1986). Although non-linear models have been proposed to address this inherent limitation of TFA (Chacon et al. 2018), the jury is still out to determine the benefits of using these models in clinical applications, and the key differences that would result in comparison with classical TFA.

The COH_{max} algorithm was tested in a large representative sample of healthy subjects, collected in previous studies with homogeneous protocols by investigators trained to the same standards. We

have opted to test the new algorithm on the effects of hypercapnia on dCA, instead of using clinical data, to allow a more rigorous evaluation based on intra-subject, with corresponding repeated-measures statistics, rather than inter-subject differences in dCA efficacy. For this reason, our results cannot be extended to other datasets, and future studies are needed to confirm our findings in different populations.

As expected, the COHmax algorithm led to increasing values of coherence with the gradual removal of segments of data. However, we cannot guarantee that the resulting values were the absolute optimal. The main reason behind this limitation was the sequential assignment of segments, as described above (*COHmax algorithm step ii*). Instead, if segments of data were removed with random starting and ending points along the recording, combined with the use of bootstrapping, there would be the possibility of achieving even higher values of coherence than we obtained.

Unusual as this might seem, our data were of better quality than what would be desirable to provide a more stringent test of COH_{max} . In clinical applications, we have observed much higher rates of rejection of ARI estimates, due to poor coherence and high values of NMSE (Caldas et al. 2017; Lam et al. 2019; Panerai et al. 2016), and it would have been informative if the dataset we analysed had a higher proportion of problematic recordings than was the case.

Our results were dependent on the choice of the 95% confidence limit of coherence, as the threshold for acceptance of TFA parameters. The choice of a different threshold, for example the 90% or 99% confidence limit (Claassen et al. 2016), would undoubtedly lead to different results. Although our confidence limits, and their dependence on the degrees of freedom, resulting from the TFA settings, were based on the use of broad band noise for input and output (Claassen et al. 2016), we have shown previously that similar results are obtained when using surrogate pairs, based on the inter-subject swap of BP and CBFV signals (Panerai et al. 2018).

Separate values of gain and phase were not presented. As mentioned in the Introduction, the ARI incorporates all the information provided by gain and phase, without the need to breakdown these estimates in averaged values for empirically selected frequency bands, usually termed, very-low and low frequency intervals (Claassen et al. 2016). Gain has not performed as reliably in detecting

alterations in dCA as phase and ARI have (Claassen et al. 2016; Intharakham et al. 2019a; Panerai 2008), and the latter two are closely linked by the influence of phase in the temporal pattern of the CBFV step response, that ultimately defines the value of ARI (Panerai 2008). Although the results reported herein for ARI are likely to be applicable to phase as well, this needs to be demonstrated by future studies.

5. Conclusions

The coherence of TFA between BP and CBFV can be increased by the selective removal of sub-segments of data, an approach that might be useful to rescue recordings that otherwise would be rejected due to values of coherence below the statistical threshold recommended for acceptance of estimates of gain, phase, or ARI index. Before COH_{max} , an algorithm that can remove sub-segments of data in automated fashion, could be recommended for routine calculation of TFA parameters, it is necessary to test its performance more widely, and also to shed light on the benefits of achieving values of coherence significantly higher than the 95% confidence level threshold usually adopted for acceptance of dynamic CA metrics derived by TFA. Further work is needed to test COH_{max} with different sets of data, mainly in recordings obtained in clinical studies where data quality can be jeopardised.

Acknowledgments

Supported by EPSRC grant EP/K041207/1. KI is supported by a PhD scholarship from the Ministry of Science and Technology, Royal Thai Government. Professor Robinson is a National Institute for Health Research (NIHR, UK) Senior Investigator. The views expressed in this article are those of the author(s) and not necessarily those of the NIHR, or the Department of Health and Social Care (UK).

Tables

Table 1 – Physiological characteristics at baseline (normocapnia) and hypercapnia (5% CO₂ breathing in air)

Variable	Normocapnia	Hypercapnia	p-value
CBFV (R) (cm/s)	54.6 ± 12.8	60.5 ± 15.1	<0.001
CBFV (L) (cm/s)	53.0 ± 12.3	60.7 ± 14.8	<0.001
Mean BP (mmHg)	90.3 ± 15.8	93.5 ± 17.8	<0.001
Systolic BP (mmHg)	128.6 ± 24.2	134.7 ± 28.1	<0.001
Diastolic BP (mmHg)	72.4 ± 10.7	76.8 ± 11.7	<0.005
Heart rate (bpm)	66.9 ± 9.7	68.1 ± 9.7	<0.001
End-tidal CO ₂ (mmHg)	39.54 ± 4.59	42.84 ± 3.91	<0.001

CBFV: cerebral blood flow velocity; R,L: right, left MCA; BP: blood pressure; p-value from paired Student's t-test.

Table 2 – Two-way ANOVA of ARI changes with increasing coherence for normocapnia and hypercapnia.

SEG _D (s)	Baseline		Hypercapnia		p-value		
	ARI	SD _{intra}	ARI	SD _{intra}	CO ₂ effect	coherence effect	interaction
100	5.79 ± 1.40 (n=91)	0.43 ± 0.38 (n=91)	4.01 ± 1.74 (n=95)	0.71 ± 0.45 (n=95)	<0.0001	0.18	0.25
50	5.84 ± 1.40 (n=84)	0.55 ± 0.40 (n=84)	4.40 ± 1.57 (n=91)	1.69 ± 0.44 (n=91)	<0.0001	0.18	0.99
25	5.66 ± 1.49 (n=83)	0.58 ± 0.37 (n=83)	4.39 ± 1.37 (n=99)	0.69 ± 0.39 (n=99)	<0.0001	<0.0001	0.94

SEG_D: Duration of segments; p-values from two-way repeated measures ANOVA for the effects of coherence and 5% CO₂ breathing (hypercapnia) on ARI. (n) is the number of subjects with complete values of ARI for all segment durations.

Table 3 – Number (%) subjects with values of ARI rejected with standard settings and the number (%) that could be recovered with the COH_{max} algorithm.

SEG _D	Normocapnia		Hypercapnia	
	Rejected [§]	Recovered [#]	Rejected [§]	Recovered [#]
100 (s)	22 (18.3 %)	8 (36.4 %)	16 (13.3 %)	11 (68.7 %)
50 (s)	20 (16.7 %)	12 (60.0 %)	12 (10.0 %)	10 (83.3 %)
25 (s)	19 (15.8 %)	12 (63.2 %)	10 (8.3 %)	5 (50.0 %)

SEG_D: segment duration; [§] percent of total population; [#] percent of cases recovered by COH_{max}.

Figures

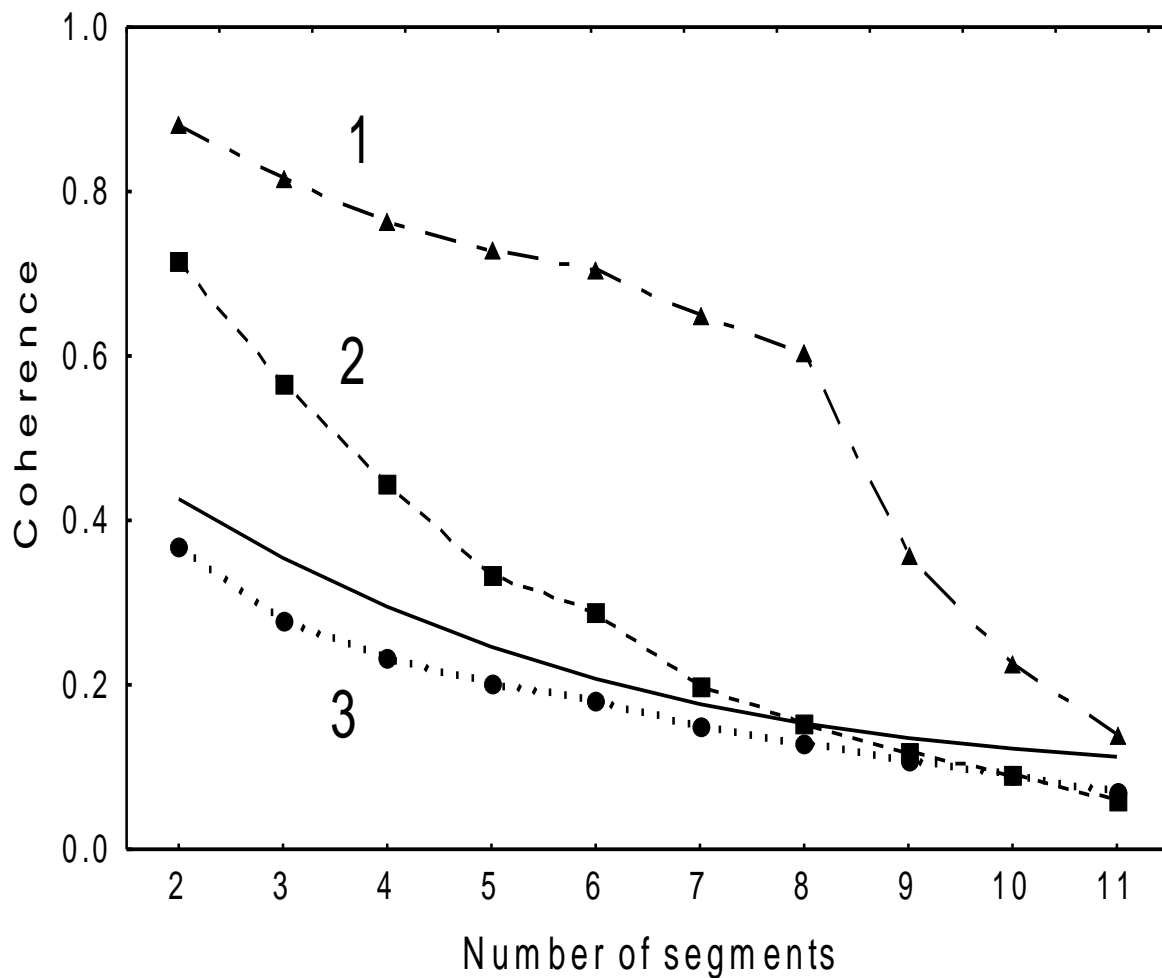


Figure 1 – Illustrative trajectories of coherence for $SEG_D = 50$ s when the number of segments is reduced from the standard value of $N_{SEG} = 11$ down to $N_{SEG} = 2$ following the COH_{max} algorithm in hypercapnia, for three different subjects. (1) rapid rise in coherence up to eight segments, followed by a more gradual rise. (2) initial value of coherence was below the 95% confidence limit (solid line), then reached the confidence limit for $N_{SEG} = 8$ and continued to rise up to $N_{SEG} = 2$. (3) despite some gradual improvement in coherence, values remained below the 95% confidence limit curve (solid line) for all values of N_{SEG} .

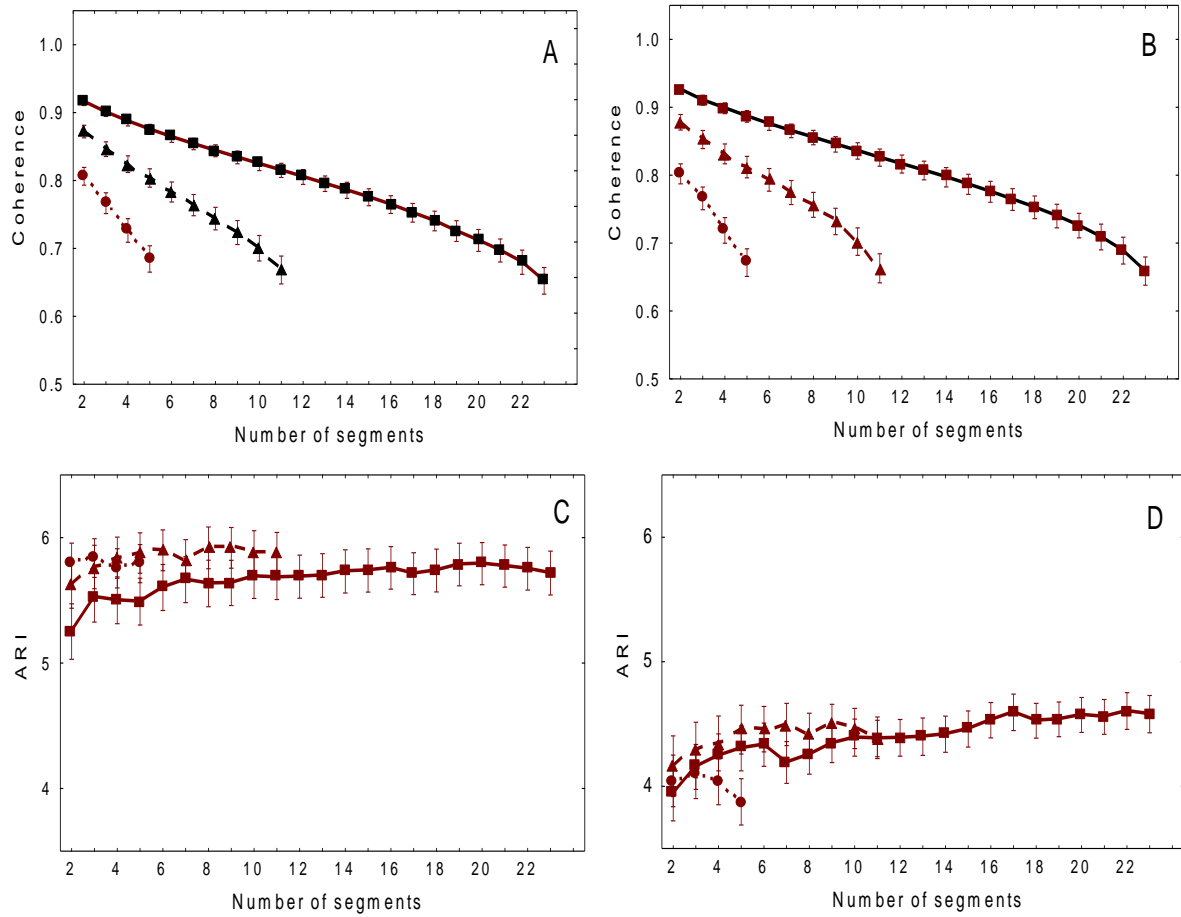


Figure 2 – Population average trajectories of coherence and the Autoregulation Index (ARI) for values of SEG_D of 25 s (squares, solid line), 50 s (triangles, dashed line) and 100 s (circles, dotted line) for normocapnia (A, C) and hypercapnia (B, D). Note the reduced scale for ARI values to facilitate visualization and its reduced values due to hypercapnia. Error bars are ± 1 SE.

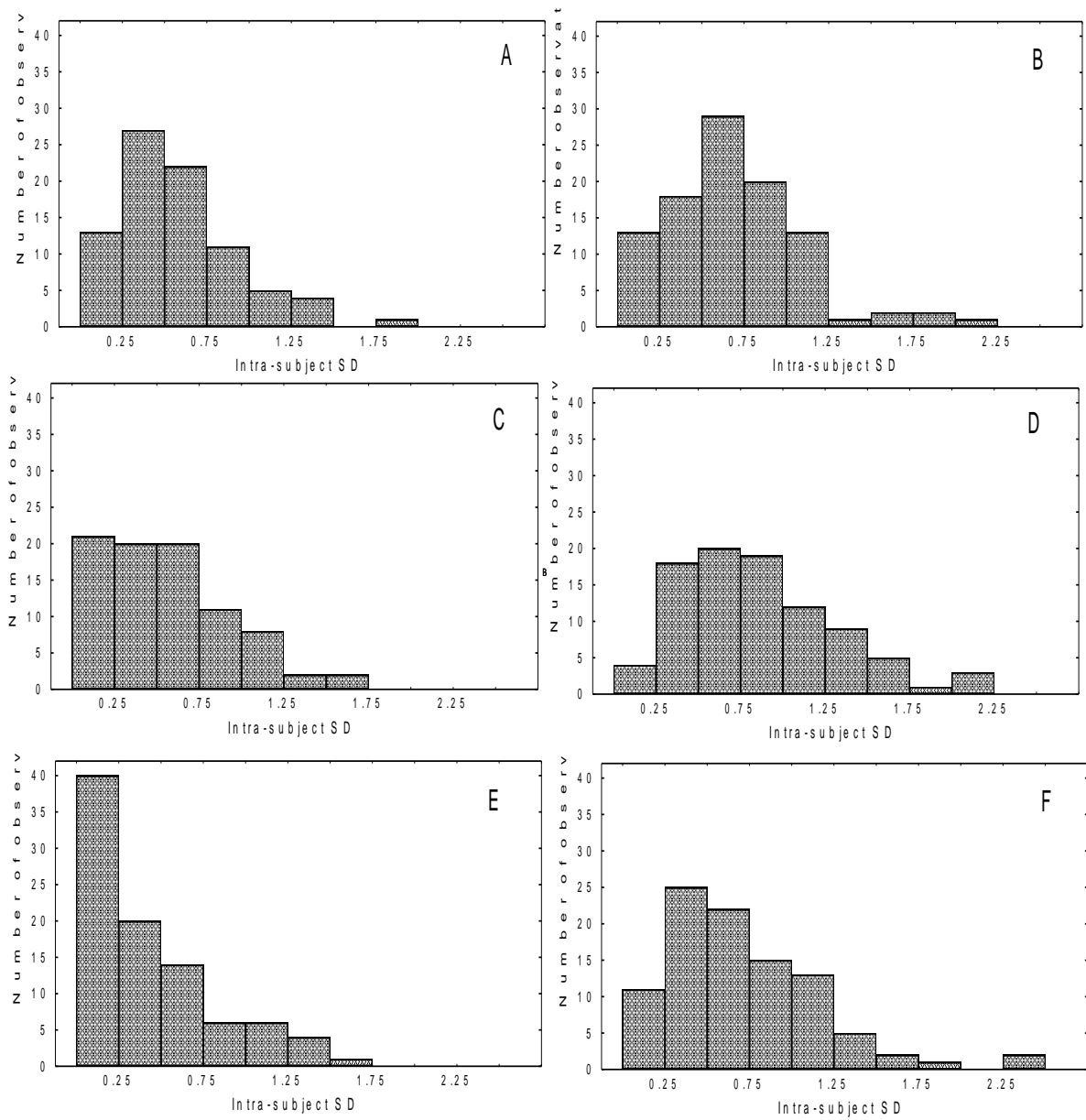


Figure 3 – Population distribution of intra-subject standard deviations (SD) for the ARI for normocapnia (A,C,E) and hypercapnia (B,D,F). (A,B) $SEG_D=25$ s, (C,D) $SEG_D=50$ s, (E,F) $SEG_D=100$ s.

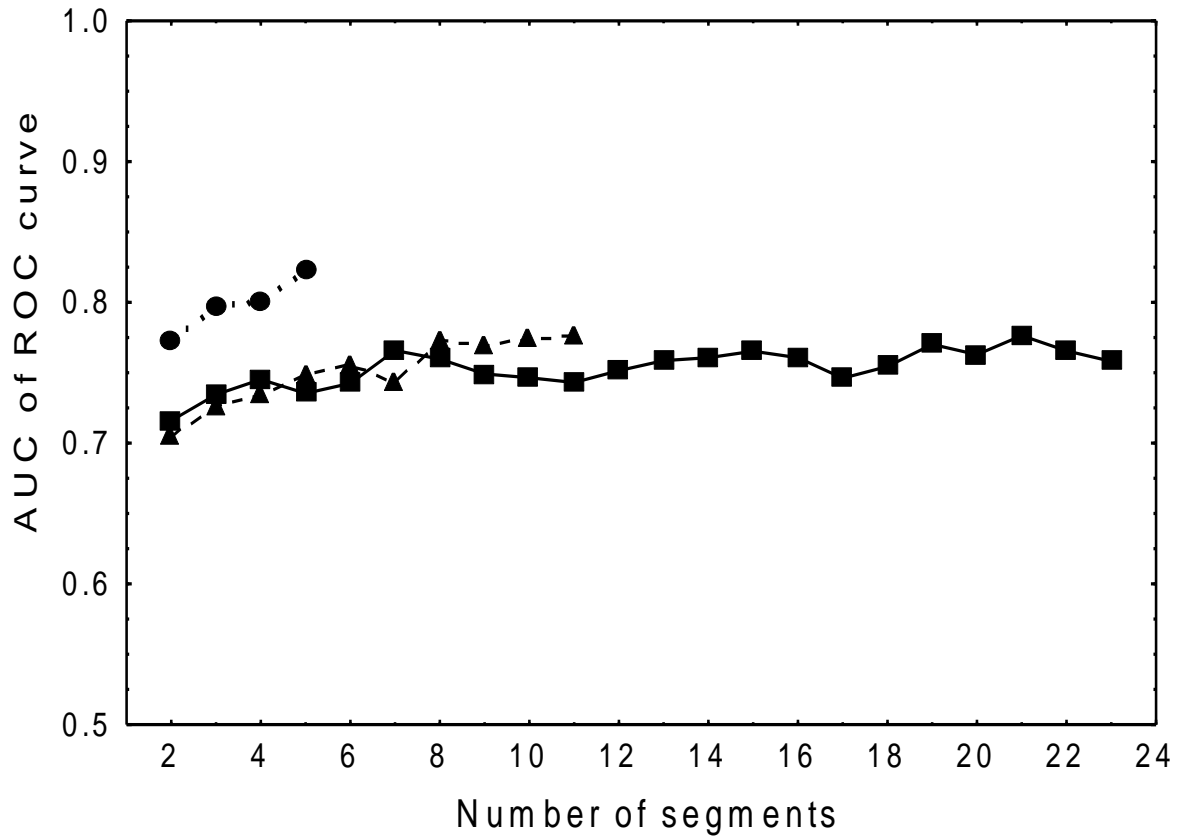


Figure 4 – Area-under-the-curve (AUC) for receiver operating characteristic (ROC) curve for detecting differences in ARI between normocapnia and hypercapnia as a function of the number of segments for $SEG_D=25$ s (squares, continuous line), 50 s (triangles, dashed line), and 100 s (circles, dotted line).

References

- Aaslid R, Lindegaard KF, Sorteberg W, and Nornes H.** Cerebral autoregulation dynamics in humans. *Stroke* 20: 45-52, 1989.
- Beishon LC, Minhas JS, Nogueira RC, Castro P, Budgeon C, Aries M, Payne SJ, Robinson TG, and Panerai RB.** INFOMATAS multi-center systematic review and meta-analysis individual patient data of dynamic cerebral autoregulation in ischemic stroke. *Int. J. Stroke* Feb 24:1747493020907003: 2020.
- Bendat JS, and Piersol AG.** *Random Data Analysis and Measurement Procedures*. New York: John Wiley & Sons, 1986, p. 1-566.
- Benignus VA.** Estimation of the coherence spectrum and its confidence interval using the fast Fourier transform. *IEEE Trans. Audio Electroacoust.* 17: 145-150, 1969.
- Brady KM, Lee JK, Kibler KK, Easley RB, Koehler RC, and Shaffner DH.** Continuous measurement of autoregulation by spontaneous fluctuations in cerebral perfusion pressure. Comparison of 3 methods. *Stroke* 39: 2531-2537, 2008.
- Budohoski KP, Reinhard M, Aries MJH, Czosnyka Z, Smielewski P, Pickard JD, Kirkpatrick PJ, and Czosnyka M.** Monitoring cerebral autoregulation after head injury. Which component of transcranial Doppler flow velocity is optimal? *Neurocrit. Care* 17: 211-218, 2012.
- Caldas JR, Panerai RB, Haunton VJ, Almeida JP, Ferreira GSR, Camara L, Nogueira RC, Bor-Seng-Shu E, Oliveira ML, Groehs RRV, Ferreira-Santos L, Teixeira MJ, Galas RRBG, Robinson TG, Jatene FB, and Hajjar LA.** Cerebral blood flow autoregulation in ischemic heart failure. *Am. J. Physiol. Regul. Integr. Comp. Physiol.* 312: R108-R113, 2017.
- Chacon M, Jara JL, Miranda R, Katsogridakis E, and Panerai RB.** Non-linear models for the detection of impaired cerebral blood flow autoregulation. *PLOS One* 13: e30191825, 2018.
- Claassen JAHR, Levine BD, and Zhang R.** Dynamic cerebral autoregulation during repeated squat-stand maneuvers. *J. Appl. Physiol.* 106: 153-160, 2009.
- Claassen JAHR, Meel-van den Abeelen ASS, Simpson DM, and Panerai RB.** Transfer function analysis of dynamic cerebral autoregulation: a white paper from the International Autoregulation Research Network (CARNet). *J. Cereb. Blood Flow Metab.* 36: 665-680, 2016.
- Coverdale NS, Gati JS, Opalevych O, Perrotta A, and Shoemaker JK.** Cerebral blood flow velocity underestimates cerebral blood flow during models hypercapnia and hypocapnia. *J. Appl. Physiol.* 117: 1090-1096, 2014.
- DeLong ER, DeLong DM, and Clarke-Pearson DL.** Comparing the areas under two or more correlated receiver operating characteristic curves: A nonparametric approach. *Biometrics* 44 837-845, 1988.
- Elting JW, Maurits NM, and Aries MJH.** Variability of the autoregulation index decreases after removing the effect of the very low frequency band. *Med. Eng. Phys.* 36: 601-606, 2014.
- Elting JW, Sanders ML, Panerai RB, Aries M, Bor-Seng-Shu E, Caicedo A, Chacon M, Gommer ED, Van Huffel S, Jara JL, Kostoglou K, Mahdi A, Marmarelis VZ, Mitsis GD, Muller M, Nikolic D, Nogueira RC, Payne SJ, Puppo C, Shin DS, Simpson DM, Tarumi T, Yeliich B, Zhang R, and Claassen JAHR.** Assessment of dynamic cerebral autoregulation in humans: is reproducibility dependent on blood pressure variability? *PLOS One* 15: e0227651, 2020.
- Giller CA.** The frequency-dependent behavior of cerebral autoregulation. *Neurosurgery* 27: 362-368, 1990.
- Hu K, Peng CK, Huang NE, Wu Z, Lipsitz LA, Cavallerano J, and Novak V.** Altered phase interactions between spontaneous blood pressure and flow fluctuations in type 2 diabetes mellitus: Nonlinear assessment of cerebral autoregulation. *Physica A* 387: 2279-2292, 2008.
- Intharakham K, Beishon LC, Panerai RB, Haunton VJ, and Robinson TG.** Assessment of cerebral autoregulation in stroke: A systematic review and meta-analysis of studies at rest. *J. Cereb. Blood Flow Metab.* 39: 2105-2116, 2019a.
- Intharakham K, Panerai RB, Katsogridakis E, Lam MY, Llwyd O, Salinet ASM, Nogueira RC, Haunton VJ, and Robinson TG.** Can we use short recordings for assessment of dynamic cerebral

autoregulation? A sensitivity analysis study in acute ischaemic stroke and healthy subjects. *Physiol. Meas.* 40: 085002, 2019b.

Katsogridakis E, Bush G, Fan L, Birch AA, Simpson DM, Allen R, Potter JF, and Panerai RB. Detection of impaired cerebral autoregulation improves by increasing arterial blood pressure variability. *J. Cereb. Blood Flow Metab.* 33: 519-523, 2013.

Lam MY, Haunton VJ, Robinson TG, and Panerai RB. Dynamic cerebral autoregulation measurement using rapid changes in head positioning: experiences in acute ischemic stroke and healthy control populations. *Am. J. Physiol. Heart Circ. Physiol.* 316: H673-H683, 2019.

Liu J, Simpson DM, and Allen R. High spontaneous fluctuations in arterial blood pressure improves the assessment of cerebral autoregulation. *Physiol. Meas.* 26: 725-741, 2005.

Llwyd O, Panerai RB, and Robinson TG. Effects of dominant and non-dominant passive arm manoeuvres on the neurovascular coupling response. *Eur. J. Appl. Physiol.* 117: 2191-2199, 2017.

Maggio P, Salinet ASM, Panerai RB, and Robinson TG. Does hypercapnia-induced impairment of cerebral autoregulation affect neurovascular coupling? A functional TCD study. *J. Appl. Physiol.* 115: 491-497, 2013.

Meel-van den Abeelen ASS, Van Beek AHEA, Slump CH, Panerai RB, and Claassen JAHR. Transfer function analysis for the assessment of cerebral autoregulation using spontaneous oscillations in blood pressure and cerebral blood flow. *Med. Eng. Phys.* 36: 563-575, 2014.

Minhas JS, Panerai RB, and Robinson TG. Modelling the cerebral haemodynamic response in the physiological range of PaCO₂. *Physiol. Meas.* 39: 1-11, 2018.

Ono M, Joshi B, Brady K, Easley RB, Zheng Y, Brown C, Baumgartner RW, and Hogue Jr CW. Risks for impaired cerebral autoregulation during cardiopulmonary bypass and postoperative stroke. *Br. J. Anaest.* 109: 391-398, 2012.

Panerai RB. Cerebral autoregulation: From models to clinical applications. *Cardiovasc. Eng.* 8: 42-59, 2008.

Panerai RB. Nonstationarity of dynamic cerebral autoregulation. *Med. Eng. Phys.* 36: 576-584, 2013.

Panerai RB, Carey BJ, and Potter JF. Short-term variability of cerebral blood flow velocity responses to arterial blood pressure transients. *Ultrasound Med. Biol.* 29: 31-38, 2003.

Panerai RB, Deverson ST, Mahony P, Hayes P, and Evans DH. Effect of CO₂ on dynamic cerebral autoregulation measurement. *Physiol. Meas.* 20: 265-275, 1999.

Panerai RB, Haunton VJ, Minhas JS, and Robinson TG. Inter-subject analysis of transfer function coherence in studies of dynamic cerebral autoregulation. *Physiol. Meas.* 39: 125006, 2018.

Panerai RB, Haunton VJ, Salinet ASM, and Robinson TG. Statistical criteria for estimation of the cerebral autoregulation index (ARI) at rest. *Physiol. Meas.* 37: 661-680, 2016.

Panerai RB, Intharakham K, Haunton VJ, Minhas JS, Llwyd O, Lam MY, Salinet ASM, Nogueira RC, Katsogridakis E, Maggio P, and Robinson TG. Chasing the evidence: the influence of data segmentation on estimates of dynamic cerebral autoregulation. *Physiol. Meas.* Mar 9: 1-10, 2020.

Panerai RB, Kelsall AWR, Rennie JM, and Evans DH. Analysis of cerebral blood flow autoregulation in neonates. *IEEE Trans. Biomed. Eng.* 43: 779-788, 1996.

Panerai RB, Kelsall AWR, Rennie JM, and Evans DH. Cerebral autoregulation dynamics in premature newborns. *Stroke* 26: 74-80, 1995.

Panerai RB, Moody M, Eames PJ, and Potter JF. Dynamic cerebral autoregulation during brain activation paradigms. *Am. J. Physiol. Heart Circ. Physiol.* 289: H1202-H1208, 2005.

Panerai RB, Rennie JM, Kelsall AWR, and Evans DH. Frequency-domain analysis of cerebral autoregulation from spontaneous fluctuations in arterial blood pressure. *Med. Biol. Eng. Comput.* 36: 315-322, 1998a.

Panerai RB, White RP, Markus HS, and Evans DH. Grading of cerebral dynamic autoregulation from spontaneous fluctuations in arterial blood pressure. *Stroke* 29: 2341-2346, 1998b.

Rivera-Lara L, Zorrilla-Vaca A, Geocadin R, Ziai W, Healy R, Thompson R, Smielewski P, Czosnyka M, and Hogue Jr CW. Predictors of outcome with cerebral autoregulation monitoring: a systematic review and meta-analysis. *Crit. Care Med.* 45: 695-704, 2017.

Robbe HWJ, Mulder LJM, Ruddle H, Langewitz WA, Veldman JBP, and Mulder G. Assessment of baroreceptor reflex sensitivity by means of spectral analysis. *Hypertension* 10: 538-543, 1987.

Sanders ML, Claassen JAHR, Aries M, Bor-Seng-Shu E, Caicedo A, Chacon M, Gommer ED, Van Huffel S, Jara JL, Kostoglou K, Mahdi A, Marmarelis VZ, Mitsis GD, Muller M, Nikolic D, Nogueira RC, Payne SJ, Puppo C, Shin DS, Simpson DM, Tarumi T, Yeliich B, Zhang R, Panerai RB, and Elting JW. Reproducibility of dynamic cerebral autoregulation parameters: a multi-centre, multi-method study. *Physiol. Meas.* 39: 125002, 2018.

Sanders ML, Elting JW, Panerai RB, Aries M, Bor-Seng-Shu E, Caicedo A, Chacon M, Gommer ED, Van Huffel S, Jara JL, Kostoglou K, Mahdi A, Marmarelis VZ, Mitsis GD, Muller M, Nikolic D, Nogueira RC, Payne SJ, Puppo C, Shin DS, Simpson DM, Tarumi T, Yeliich B, Zhang R, and Claassen JAHR. Dynamic cerebral autoregulation reproducibility is affected by physiological variability. *Front. Physiol.* 10: 865, 2019.

Saul JP, Berger RD, Albrecht P, Stein SP, Chen MH, and Cohen RJ. Transfer function analysis of the circulation: unique insights into cardiovascular regulation. *Am J. Physiol. Heart Circ. Physiol.* 261: H1231-H1245, 1991.

Simpson DM, and Claassen J. CrossTalk opposing view: dynamic cerebral autoregulation should be quantified using induced (rather than spontaneous) blood pressure fluctuations. *J. Physiol.* 596: 7-9, 2018.

Smirl JD, Haykowsky MJ, Nelson MD, Tzeng YC, Marsden KR, Jones H, and Ainslie PN. Relationship between cerebral blood flow and blood pressure in long-term heart transplant recipients. *Hypertension* 64: 1314-1320, 2014.

Smirl JD, Hoffman K, Tzeng YC, Hansen AE, and Ainslie PN. Methodological comparison of active- and passive-driven oscillations in blood pressure: implications for the assessment of cerebral pressure-flow relationships. *J. Appl. Physiol.* 119: 487-501, 2015.

Tiecks FP, Lam AM, Aaslid R, and Newell DW. Comparison of static and dynamic cerebral autoregulation measurements. *Stroke* 26: 1014-1019, 1995.

Tzeng YC, and Panerai RB. CrossTalk proposal: dynamic cerebral autoregulation should be quantified using spontaneous blood pressure fluctuations. *J. Physiol.* 596: 3-5, 2018.

Verbree J, Bronzwaer ASGT, Ghariq E, Versluis MJ, Daemen MJAP, van Buchem MA, Dahan A, van Lieshout JJ, and van Osch MJP. Assessment of middle cerebral artery diameter during hypocapnia and hypercapnia in humans using ultra-high-field MRI. *J. Appl. Physiol.* 117: 1084-1089, 2014.

Welch PD. The use of the Fast Fourier Transform for the estimation of power spectra: a method based on time averaging over short, modified periodograms. *IEEE Trans. Audio Electroacoust.* 15 70-73, 1967.

Zhang R, Zuckerman JH, Giller CA, and Levine BD. Transfer function analysis of dynamic cerebral autoregulation in humans. *Am. J. Physiol. Heart Circ. Physiol.* 274: H233-H241, 1998.